



Interannual variations of water vapor in the tropical upper troposphere and the lower and middle stratosphere and their connections to ENSO and QBO

Edward W Tian^{1,2}, Hui Su¹, Baijun Tian¹, and Jonathan H. Jiang¹

5 ¹Jet Propulsion Laboratory, California Institute of Technology, Pasadena, CA, USA

²Department of Economics, University of California, Santa Cruz, CA, USA

Correspondence to: Dr. Jonathan Jiang (Jonathan.H.Jiang@jpl.caltech.edu)

Abstract. In this study, we analyze the Aura Microwave Limb Sounder water vapor data in the tropical upper troposphere and the lower and middle stratosphere (UTLMS) (from 215 hPa to
10 6 hPa) for the period from August 2004 to September 2017 using time-lag regression analysis and composite analysis to explore the interannual variations of tropical UTLMS water vapor and their connections to El Niño Southern Oscillation (ENSO) and quasi-biennial oscillation (QBO). Our analysis shows that ENSO's impact on the interannual tropical water vapor anomalies is strong in the upper troposphere (~215 to ~120 hPa) and near the tropopause (~110
15 to ~90 hPa) with a ~3-month lag but weak in the lower and middle stratosphere (~80 to ~6 hPa). In contrast, QBO has a large impact on the interannual tropical water vapor anomalies in the lower and middle stratosphere with an upward propagating signal starting at the tropopause (100 hPa), peaking first in the lower stratosphere near 68 hPa with a ~7-month lag and then in the middle stratosphere near 15 hPa with a ~24-month lag. The phase lag is based on the 30-
20 hPa QBO index and should be different from that found by previous studies based on the 50-hPa QBO index. In the upper troposphere, interannual tropical water vapor anomalies are positive during the warm ENSO phases but negative during the cold ENSO phases no matter what QBO phases are. Near the tropopause, interannual tropical water vapor anomalies are different depending on different ENSO and QBO phase combinations. In the lower and middle



stratosphere, interannual tropical water vapor anomalies are mainly determined by QBO instead of ENSO. For the easterly QBO phases, interannual tropical water vapor anomalies are positive in the lower stratosphere but negative in the middle stratosphere. Vice versa for the westerly QBO phases.

5 1 Introduction

Water vapor (WV) is the dominant greenhouse gas in the atmosphere and plays an important role in global weather and climate systems. Since higher temperature is associated with higher saturation vapor pressure, water vapor has a positive feedback to surface warming. Previous studies indicate that the water vapor feedback is the largest positive feedback in climate models that increases the sensitivity of surface temperature to increasing carbon dioxide (Held and Soden, 2000; Soden and Held, 2006). The middle and upper tropospheric water vapor dominates the water vapor feedback (Held and Soden, 2000; Soden et al., 2008). The stratospheric water vapor may account for about 10% of total water vapor feedback (Dessler et al., 2013). In addition, the water vapor in the stratosphere plays an important role in stratospheric ozone chemistry and global radiative balance (Forster and Shine, 1999; Solomon et al., 2010). Thus, it is important to study the water vapor variability in the upper troposphere and the lower and middle stratosphere (UTLMS).

Large interannual variations of water vapor in the tropical UTLMS have been observed and shown to be important for both climate and chemical reasons (e.g., Dessler et al., 2013; 2014; Fueglistaler and Haynes, 2005; Liang et al., 2011; Liess and Geller, 2012; Randel and Jensen, 2013; Tao et al., 2015; Ye et al., 2018). Several well-known interannual climate modes are found to modulate the interannual variations of tropical UTLMS water vapor, such as the El Niño Southern Oscillation (ENSO) (e.g., Dessler et al., 2014; Liang et al., 2011; Randel et al.,



2004; Ye et al., 2018), the quasi-biennial oscillation (QBO) (e.g., Dessler et al., 2014; Fueglistaler and Haynes, 2005; Geller et al., 2002; Liang et al., 2011; Liess and Geller, 2012; Randel et al., 2004; Randel and Jensen, 2013; Tao et al., 2015; Ye et al., 2018), and the Brewer–Dobson circulation (BDC) (e.g., Dessler et al., 2013; 2014). ENSO is the interannual oscillation
5 of sea surface temperatures (SSTs) and easterly trade winds in the tropical Pacific oceans caused by the coupled interactions between the ocean and atmosphere (Wallace et al., 1998). It is the primary source of global interannual climate variabilities (Philander, 1990; Wallace et al., 1998). During a warm ENSO (El Nino) phase, trade winds are weaker and warm waters move eastward to the equatorial central and eastern Pacific. During a cold ENSO (La Nina)
10 phase, trade winds are stronger and warm waters move further westward to the equatorial western Pacific. QBO describes the quasi-biennial oscillation of downward propagating easterly or westerly zonal winds in the equatorial stratosphere with a period of ~28 months (Baldwin et al., 2001). It is well known that QBO causes large-scale circulation changes that affect ozone, water vapor, methane and global weather and climate (Baldwin et al., 2001).
15 ENSO can modulate the tropical UTLMS water vapor through several physical and dynamical processes, such as convective transport of tropospheric water vapor, evaporation of cloud ice, and the perturbations of tropical tropopause (~100 hPa) temperature (e.g., Dessler et al., 2014; Gettelman et al., 2001; Liang et al., 2011; Ye et al., 2018; Zhou et al., 2001, 2004). On the other hand, the QBO's impact on the tropical UTLMS water vapor is mainly through the QBO's
20 influence on the tropical tropopause temperature that regulates the amount of upper tropospheric water vapor entering the stratosphere (e.g., Fueglistaler et al., 2009; Liang et al., 2011; Randel et al., 2004; Zhou et al., 2001, 2004).

Dessler et al. (2013; 2014) performed a multi-linear regression of the tropical lower
25 stratospheric (82-hPa) water vapor variability to the QBO, BDC and tropospheric temperature (which is correlated with ENSO). They found that the tropical lower stratospheric water vapor



lags QBO by about 3 months and lags BDC by 1 month based on the 50-hPa QBO index. Ye et al. (2018) performed a two-dimensional multivariate linear regression of the tropical tropopause water vapor interannual variability to the QBO, BDC and tropospheric temperature as a function of latitude and longitude. They found that the evaporation of convective ice from increased deep convection as the troposphere warms plays an important role in the tropopause water vapor variability in addition to changing tropopause temperature. Ding and Fu (2018) found that the tropical central Pacific SST warming contributes significantly to enhanced convection and thus sudden drop of the lower stratospheric (83-hPa) water vapor around 2000. They suggested that the tropical central Pacific SST is another important driver of the lower stratospheric water vapor variability on inter-decadal time scales. However, the aforementioned studies mainly focused on a specific level of the UTLMS layer, either 82 hPa or 100 hPa. A comprehensive investigation of the interannual variations of the tropical water vapor in the whole UTLMS layer and their relationships to ENSO and QBO is still lacking. Liang et al. (2011) performed a study with such an objective using merged Aqua Atmospheric Infrared Sounder (AIRS) and Aura Microwave Limb Sounder (MLS) temperature and water vapor record but the data record was relatively short (August 2004 to March 2010) in that study.

On the other hand, current state-of-the-art climate models have difficulties in reproducing the observed UTLMS water vapor spatial and temporal variations (e.g., Jiang et al., 2012; John and Soden, 2007; Takahashi et al., 2016; Tian et al., 2004; 2013). Large differences in the UTLMS water vapor have also been found between the satellite observations and the state-of-the-art reanalyses (Jiang et al., 2015). This implies that some fundamental physical or dynamical processes controlling the UTLMS water vapor and its variability are not well represented or even missing in the climate models and reanalyses.



This study seeks to investigate the interannual variations of water vapor in the tropical UTLMS layer (from 215 hPa to 6 hPa) and their relationships to the two well-known interannual climate modes, i.e., ENSO and QBO, using the Aura MLS UTLMS water vapor data of much longer length (August 2004 to September 2017) than previous studies, in order to better understand
5 the physical and dynamical processes that control the tropical UTLMS water vapor and its variability.

The rest of this paper is organized as follows. Section 2 describes the MLS water vapor data and the analysis methods. Section 3 presents the results followed by summary and conclusions
10 in Section 4.

2 Data and Methods

We use Version 4.2 Level 2 daily Aura MLS water vapor volume mixing ratio product as described in Read et al. (2007) and Livesey (2015) from 215 hPa to 6 hPa over the period of August 2004 to September 2017. The MLS water vapor data were averaged to monthly means
15 and gridded onto 2.5x2.5 horizontal spatial grids. The MLS Level 2 data have a vertical resolution of ~3 km and horizontal resolutions of ~7 km across track and ~200–300 km along track. The useful altitude ranges are at pressure (p) \leq 316 hPa but we only use the water vapor data above 215 hPa because of larger uncertainty below 215 hPa altitude. The measurement uncertainties (including biases) are 20% in the upper troposphere ($p > 100$ hPa) and 10% near
20 the tropopause (~100 hPa) and in the stratosphere ($p \leq 100$ hPa) (Read et al., 2007). The Aura MLS water vapor data have been used extensively in atmospheric process analysis studies and climate model evaluations (e.g., Dessler et al., 2013; 2014; Flury et al., 2012; Jiang et al., 2012; Liang et al., 2011; Liu et al., 2018; Solomon et al., 2010; Su et al., 2006; Takahashi et al., 2016;



Uma et al., 2014; Wu et al., 2012). The MLS water vapor data are freely available through the Aura MLS project website (<https://mls.jpl.nasa.gov>).

Since we are mainly interested in the tropical UTLMS, we first averaged the MLS monthly
5 water vapor data between 15°S/N , and along the entire latitude band ($wv_{t,p}$). Then, the tropical
mean seasonal cycle ($wv_{m,p}$, 12 months) was calculated as the averages of the tropical MLS
monthly water vapor data at each calendar month over the whole MLS data record. Next, de-
seasonalized monthly tropical water vapor anomalies were obtained by removing the tropical
mean seasonal cycle from the tropical monthly water vapor data ($wv'_{t,p} = wv_{t,p} - wv_{m,p}$). Then,
10 the interannual (2-7 years) tropical water vapor anomalies (or short-handed as anomalies for
simplicity) were isolated through the difference between the 12-month and 42-month running
means of the de-seasonalized monthly tropical water vapor anomalies. to remove the high-
frequency (e.g., synoptic, seasonal, intraseasonal, and annual) and low-frequency (e.g., solar
cycle and decadal) variabilities (e.g., Ding and Fu, 2018; Mote et al., 1996; Schieferdecker et
15 al., 2015; Schwartz et al., 2008; Solomon et al., 2010). Last, the interannual monthly tropical
water vapor anomalies were converted into percentage deviations through dividing the
interannual monthly tropical water vapor anomalies by the long-term tropical mean (wv_p) at
the respective pressure level. The resulting interannual monthly tropical water vapor anomalies
in percentage deviations are used throughout the analysis.

20

To represent ENSO phases, we use a bimonthly multivariate ENSO index (MEI) from National
Oceanic and Atmospheric Administration (NOAA) (<https://www.esrl.noaa.gov/psd/enso/mei/>).
The MEI is based on sea-level pressure, zonal and meridional surface winds, sea surface
temperature, surface air temperature, and total cloudiness (Wolter and Timlin, 2011). Positive
25 MEI values indicate warm ENSO (El Nino) phases while negative MEI values indicate cold
ENSO (La Nina) phases. For QBO, we use the monthly 30-hPa zonal mean zonal wind at the



Equator (u_{30}) from NOAA (<https://www.esrl.noaa.gov/psd/data/correlation/qbo.data>) based on the NCEP/NCAR reanalysis. Positive u_{30} values denote westerly QBO phases while negative u_{30} values denote easterly QBO phases. There is a ~ 3 -month phase lag between the QBO index at 30 hPa and the QBO index based on the monthly 50-hPa zonal mean zonal wind at the Equator used by other studies (Dessler et al., 2013; Dessler et al., 2014; Ye et al., 2018). Thus, the phase lag between the UTLMS water vapor anomalies and QBO in this study should be different from those found by previous studies based on the 50-hPa QBO index. The ENSO and QBO indices from August 2004 to September 2017 are shown in Fig. 1.

With the ENSO, QBO, and MLS data sets we conducted two types of analysis: lead-lag regression analysis and composite analysis. The lead-lag regression identifies how much time lag exists between the perturbation of a climate mode and the response of the UTLMS water vapor anomalies at different pressure levels. We normalized each index by dividing each index anomaly by its standard deviation before performing the linear regressions. For every pressure level and time shift, a univariate linear regression is performed first with respect to either ENSO or QBO index individually ($WV = X_0 + X_1 \times \text{ENSO}$ and $WV = X_0 + X_1 \times \text{QBO}$). The respective R-squared value of each linear regression, a standard measure of explained variance, is used to indicate how much water vapor variability can be described by each regression separately for each pressure level and time lag. The maximum R-squared value will determine the optimal time lag for the univariate linear regression at each pressure level. A multivariate linear regression with respect to ENSO and QBO together is then performed using the optimal time lags obtained from the univariate linear regressions to estimate how much water vapor variability can be described by ENSO and QBO combined. The residual between the original observation and the multivariate linear regression with respect to ENSO and QBO together is also calculated to quantify how much water vapor variability that cannot be explained by ENSO and QBO.



For the composite analysis, we first partitioned the interannual monthly MLS water vapor anomalies into four different cases based on different combinations of ENSO and QBO phases: warm ENSO ($MEI > 0.3$) and westerly QBO ($u_{30} > 3 \text{ m s}^{-1}$) case, warm ENSO ($MEI > 0.3$) and easterly QBO ($u_{30} < -3 \text{ m s}^{-1}$) case, cold ENSO ($MEI < -0.3$) and westerly QBO ($u_{30} > 3 \text{ m s}^{-1}$) case, and cold ENSO ($MEI < -0.3$) and easterly QBO ($u_{30} < -3 \text{ m s}^{-1}$) case. These threshold values were chosen in order to remove the ENSO and QBO neutral phases and have sufficient samples for the composites at the same time. We then averaged the interannual monthly MLS water vapor anomalies for each case to create a composite mean profile. The composite analysis was applied to the MLS interannual water vapor anomaly data for annual means, the summer months (MJJASO) average and the winter months (NDJFMA) average separately.

3 Results

Figure 2 shows the interannual monthly tropical water vapor anomalies from MLS in percentage deviations at different pressure levels from August 2004 to September 2017. In the upper troposphere from $\sim 215 \text{ hPa}$ to $\sim 120 \text{ hPa}$, large vertically oriented tropical water vapor anomalies of $\pm 15\%$ are evident. They seem to be coincident with several El Niño or La Niña events shown in Fig. 1 with positive anomalies during the warm ENSO phases and negative anomalies during the cold ENSO phases. In the lower and middle stratosphere ($100\text{--}6 \text{ hPa}$), large tropical water vapor anomalies of $\pm 15\%$ are found to propagate upward at a speed of about 7 km per year starting around 100 hPa with a first local maximum in the lower stratosphere around 68 hPa and a second local maximum in the middle stratosphere around 15 hPa . These have been referred to as the interannual variability of the stratospheric water vapor tape recorder (e.g., Geller et al., 2002; Liang et al., 2011) and may be regulated by QBO. The



small interannual water vapor anomalies at the first and last several months of the data record are results of the limitation of the band pass filter.

To show the relative importance of ENSO and QBO and their roles in the interannual tropical
5 water vapor anomalies at different pressure levels, Figure 3 shows the R-squared values for the
linear regressions between the MLS tropical UTLMS interannual monthly water vapor
anomalies and the ENSO or QBO index from 215 hPa to 6 hPa with time lag shifts from 0-24
months. Figure 3a (left) is for ENSO ($WV = X_0 + X_1 \times \text{ENSO}$) and Fig. 3b (right) is for QBO
($WV = X_0 + X_1 \times \text{QBO}$). The time lag shift indicates the number of months that the tropical
10 water vapor anomalies lag the ENSO or QBO index. The maximum time lag of 24 months was
chosen due to the fact that 24 months are close to the period of a QBO cycle and the minimum
period of an ENSO cycle. Figure 3a indicates the R-squared value for the linear regressions
between the tropical water vapor anomalies and the ENSO index is large (~50%) in the upper
troposphere, becomes smaller (~10%) at the tropopause (~100 hPa) and is very small (close to
15 zero) in the stratosphere above 80 hPa. This is consistent with the large vertically oriented
water vapor anomalies of $\pm 15\%$ in the upper troposphere that are coincident with several El
Nino or La Nina events shown in Fig. 2. This implies that ENSO has a strong impact on the
water vapor interannual variability in the upper troposphere and around the tropopause, while
its impact on the water vapor interannual variability is very small in the stratosphere. The
20 current finding of the strong impact of ENSO on the water vapor in the upper troposphere and
around the tropopause is consistent with several previous studies (Dessler et al., 2014; Liang
et al., 2011; Ye et al., 2018) that suggested ENSO can strongly modulate the upper tropospheric
water vapor through the convective transport of tropospheric water vapor and the evaporation
of cloud ice. In terms of the response time, the highest correlation is at ~3-month lag. This is
25 comparable to the tropospheric temperature response time to the ENSO SST anomaly (Su et
al., 2005). The current finding of the weak influence of ENSO on the water vapor anomalies in



the lower and middle stratosphere is also consistent with a previous study (Ding and Fu, 2018) that suggested the small effect of ENSO on tropical mean lower stratospheric water vapor is due to the opposite phases of lower stratospheric water vapor anomalies in response to ENSO in the longitudinal direction. This is due to the compensating effect of ENSO on the tropical tropopause temperature anomalies between the western equatorial Pacific and the central equatorial Pacific found by Liang et al. (2011).

For the linear regressions between the interannual tropical water vapor anomalies and the QBO index, Figure 3b indicates that the QBO influence is small in the upper troposphere but large in the lower and middle stratosphere. The high correlation between the tropical water vapor anomalies and the 30-hPa QBO index starts at the tropopause at a time lag of 2-3 months and propagates upwards, peaking first in the lower stratosphere at ~68 hPa at a time lag of ~7 months and then in the middle stratosphere at ~15 hPa with a time lag of ~24 months. The peak at ~15 hPa with a time lag of ~12 months is the result of the upward propagating signal starting at the tropopause at a time lag of a few months earlier than the 30-hPa QBO index. This suggests that the QBO's impacts on the stratospheric water vapor might be from its modulation on the tropical tropopause temperature, as suggested by many previous studies (e.g., Fueglistaler et al., 2009; Liang et al., 2011; Randel et al., 2004; Zhou et al., 2001, 2004). This is consistent with the upward propagating tropical water vapor anomalies of $\pm 15\%$ in the lower and middle stratosphere shown in Fig. 2 and referred to as the interannual variability of the stratospheric water vapor tape recorder (e.g., Geller et al., 2002; Liang et al., 2011). This indicates that the interannual variability of the stratospheric water vapor tape recorder (e.g., Geller et al., 2002; Liang et al., 2011) is a result of the impact of QBO.

Figure 4 shows the time series of the monthly interannual tropical MLS water vapor anomalies (blue lines) and the predicted interannual monthly tropical water vapor anomalies based on the



univariate linear regressions on the ENSO index only (red lines) or the QBO index only (orange lines) at the time lag less than 12 months with the highest R-squared value for four specific pressure levels: 147-hPa, 100-hPa, 68-hPa, 15-hPa, representing the upper troposphere, tropopause, lower stratosphere, and mid-stratosphere, respectively. Figure 4 reaffirms the results shown in Fig. 3: the decreasing contributions of ENSO and the increasing contributions of QBO to the interannual variability of UTLMS water vapor as the altitude increases. The R-squared value for the linear regressions between the MLS interannual tropical water vapor anomalies and the ENSO index is ~54% at the 147-hPa altitude with a ~3-month time lag, ~8% at the tropopause with a ~11-month time lag, and decreases to ~1% at the 68-hPa altitude with a ~12-month time lag and ~2% at the 15-hPa altitude with a ~6-month time lag. In contrast, the R-squared value for the linear regressions between the MLS interannual tropical water vapor anomalies and the QBO index is small (~5%) at the 147-hPa altitude with a ~0-month time lag, becomes significant (~38%) at the tropopause with a ~5-month time lag, reaches the first maximum (~44%) at the 68-hPa altitude with a ~8-month time lag and the second maximum (~60%) at the 15-hPa altitude with a ~11-month time lag. Therefore, the interannual variability of the UTLMS tropical water vapor is mainly modulated by ENSO instead of QBO in the upper troposphere (from ~215 hPa to ~120 hPa), by both ENSO and QBO around the tropopause (from ~110 hPa to ~90 hPa), and by mainly QBO instead of ENSO in the lower and middle stratosphere (from ~80 hPa to 6 hPa).

20

Figure 4 also shows the predicted monthly interannual tropical water vapor anomalies based on the multivariate linear regressions on the ENSO and QBO indices together (purple lines) and the differences (green lines) between the original MLS interannual monthly tropical water vapor anomalies (blue lines) and the multivariate linear regression (purple lines) at the four specific pressure levels. Fig. 4 indicates that the predicted interannual monthly tropical water vapor anomalies based on the multivariate linear regressions of ENSO and QBO are very

25



similar to the original MLS interannual monthly tropical water vapor anomalies. ENSO and QBO together can explain most variance of the interannual monthly tropical water vapor anomalies, ~56% at the 147-hPa altitude, ~43% at the tropopause, ~44% at the 68-hPa altitude, and ~60% at the 15-hPa altitude. However, large residues are still evident in Fig. 4 indicating that other processes, such as the BDC, in addition to ENSO and QBO has to be considered in order to explain the full interannual variability of the tropical UTLMS water vapor. This issue is beyond the scope of this paper and will be investigated in the future.

To highlight the different roles of ENSO and QBO phases in the interannual tropical water vapor anomalies at different pressure levels and different seasons, Figure 5 shows the composite interannual tropical water vapor anomalies from MLS as function of pressure levels for winter (NDJFMA) (blue lines), summer (MJJASO) (red lines), and annual (black lines) means at four different cases based on different combinations of ENSO and QBO phases. Consistent with Figs. 3 and 4, Figure 5 shows that ENSO mainly impacts the interannual tropical water vapor anomalies in the upper troposphere and at the tropopause, while QBO mainly affects the interannual tropical water vapor anomalies at the tropopause and in the lower and middle stratosphere. In the upper troposphere (215-120 hPa), the interannual tropical water vapor anomalies are mainly determined by the ENSO phase and its seasonal change while the QBO's effect is negligible. For example, positive interannual tropical water vapor anomalies are found during the warm ENSO phases, while negative interannual tropical water vapor anomalies are found during the cold ENSO phases for the annual, winter and summer means no matter what QBO phases are. The interannual tropical water vapor anomalies tend to larger during the winter than during the summer because the ENSO events are usually stronger during the winter than during the summer (Wallace et al., 1998). During the La Nina cases, it seems that easterly QBO tends to reduce the magnitudes of the negative interannual tropical water



vapor anomalies. For example, the averaged interannual tropical water vapor anomalies in the upper troposphere for the summer and the cold easterly QBO case are rather small.

Near the tropopause (110-90 hPa), both ENSO and QBO as well as their season changes can influence the interannual tropical water vapor anomalies. Both warm ENSO phase and westerly QBO phase tend to cause positive interannual tropical water vapor anomalies while cold ENSO phase and easterly QBO phase tend to cause negative interannual tropical water vapor anomalies in this layer. As a result, different interannual tropical water vapor anomalies are found for different cases depending the different ENSO and QBO phase combinations and their seasonal variations in this layer (Liang et al., 2011). For example, very strong positive interannual tropical water vapor anomalies are found for the warm westerly case and very strong negative interannual tropical water vapor anomalies are found for the cold easterly case due to the supporting effect of ENSO and QBO for the winter season. Weak interannual tropical water vapor anomalies are found for the warm easterly case and the cold westerly case due to the compensating effect of ENSO and QBO.

In the lower and middle stratosphere (80-6 hPa), QBO and its seasonal change dominate the interannual tropical water vapor anomalies while the ENSO's effect seems to be negligible. QBO explains ~50-60%, in contrast to ~2% by ENSO, of the tropical water vapor interannual variance. During the westerly QBO phases, interannual tropical water vapor anomalies are positive near the tropopause, negative in the lower stratosphere (below ~30-hPa altitude), and positive again in the middle stratosphere (above ~30-hPa altitude) for all seasons. The opposite occurs during the easterly QBO phases. The sign reversal of the interannual tropical water vapor anomalies along the pressure levels in Fig. 5 are consistent with the upward propagating water vapor anomalies and the R-squared values shown in Figs. 2 and 3b. There are some



differences in interannual tropical water vapor anomalies between warm and cold ENSO phases and between the summer and winter seasons, but they are relatively small.

4 Summary and Conclusions

In this study, we have analyzed the Aura MLS tropical UTLMS monthly water vapor data from 5 215 hPa to 6 hPa and from August 2004 to September 2017 using time-lag regression analysis and composite analysis to explore the interannual variations of water vapor in the whole tropical UTLMS layer and their connections to ENSO and QBO. The main findings of our analysis are summarized below.

10 The interannual variability of the tropical UTLMS water vapor is mainly modulated by ENSO instead of QBO in the upper troposphere (from ~215 hPa to ~120 hPa), by both ENSO and QBO around the tropopause (from ~110 hPa to ~90 hPa), and by QBO instead of ENSO in the lower and middle stratosphere (from ~80 hPa to ~6 hPa).

15 In the upper troposphere (215-120 hPa), the interannual tropical water vapor anomalies are primarily determined by ENSO and its seasonal change with a ~3-month time lag while the QBO's effect is negligible. ENSO explains ~55%, in contrast to ~5% by QBO, of the interannual tropical water vapor variance. ENSO modulates the upper tropospheric water vapor mainly through the convective transport of tropospheric water vapor and the evaporation of 20 cloud ice. Positive interannual tropical water vapor anomalies are found during the warm ENSO phases, while negative interannual tropical water vapor anomalies are found during the cold ENSO phases for all seasons although the interannual tropical water vapor anomalies tend to larger during the winter than during the summer.



Near the tropopause (110-90 hPa), both ENSO and QBO as well as their seasonal changes are important for the interannual tropical water vapor anomalies. ENSO explains ~8% while QBO explains ~38% of the interannual tropical water vapor variance. QBO modulates the tropical tropopause water vapor mainly by its modulation of the tropical tropopause temperature. Both
5 warm ENSO phase and westerly QBO phase tend to cause interannual tropical positive water vapor anomalies while cold ENSO phase and easterly QBO phase tend to cause negative interannual tropical water vapor anomalies. As a result, different interannual tropical water vapor anomalies are found for different combinations of ENSO and QBO phases and their seasonal variations.

10

In the lower and middle stratosphere (80-6 hPa), QBO and its seasonal change dominate the interannual monthly water vapor anomalies while the ENSO's effect is negligible. QBO explains ~50-60%, in contrast to ~2% by ENSO, of the interannual tropical water vapor variance. During the westerly QBO phase, interannual tropical water vapor anomalies are
15 positive near the tropopause, negative in the lower stratosphere (below ~30-hPa altitude), and positive again in the middle stratosphere (above ~30-hPa altitude) for all seasons. The opposite occurs during the easterly QBO phase. There are some small differences in interannual tropical water vapor anomalies between warm and cold ENSO phases and between the summer and winter seasons.

20

In summary, ENSO has a strong impact on the interannual variations of tropical water vapor below 90-hPa altitude, i.e., in the upper troposphere and at the tropopause. On the other hand, QBO has a large impact on the interannual variations of tropical water vapor above 110-hPa, i.e., at the tropopause and in the lower and middle stratosphere. ENSO and QBO together can
25 explain most but not all the interannual variations of the tropical UTLMS water vapor. Other



processes, such as the BDC, has to be considered in order to fully explain the interannual variability of the tropical UTLMS water vapor.

The findings in the current study are generally consistent with those from previous studies (e.g.,
5 Dessler et al., 2014; Ding and Fu, 2018; Liang et al., 2011; Ye et al., 2018). However, the relative role of ENSO and QBO on the tropical UTLMS water vapor interannual variabilities for the entire UTLMS layer and at different phase lags are more completely investigated in the current study than the previous ones. These results can serve as an important benchmark for future climate model evaluation studies.

10 **Data availability**

The MLS water vapor data used in this research are freely available through the Aura MLS project website (<https://mls.jpl.nasa.gov>). The multivariate ENSO indices used in this research are freely available from the NOAA website (<https://www.esrl.noaa.gov/psd/enso/mei/>). The QBO indices used in this research are also freely available from the NOAA website
15 (<https://www.esrl.noaa.gov/psd/data/correlation/qbo.data>).

Author contributions

JHJ, HS, and BT designed this study. EWT performed the data analysis and prepared the figures. All authors contributed to the discussion of the findings and the preparation of the manuscript.

Competing interests

20 The authors declare that they have no conflict of interests.



Acknowledgments

This research was performed at Jet Propulsion Laboratory, California Institute of Technology (Caltech), under a contract with National Aeronautics and Space Administration. It was supported by the Aura Microwave Limb Sounder project. The first author thanks Matthew Worden for his help with the MATLAB code. Caltech Copyright 2018. All rights reserved.

References

- Baldwin, M. P., Gray, L. J., Dunkerton, T. J., Hamilton, K., Haynes, P. H., Randel, W. J., Holton, J. R., Alexander, M. J., Hirota, I., Horinouchi, T., Jones, D. B. A., Kinniersley, J. S., Marquardt, C., Sato, K., and Takahashi, M.: The quasi-biennial oscillation, *Rev. Geophys.*, 39, 179-229, doi:10.1029/1999rg000073, 2001.
- Dessler, A. E., Schoeberl, M. R., Wang, T., Davis, S. M., and Rosenlof, K. H.: Stratospheric water vapor feedback, *Proc. Nat. Acad. Sci. USA*, 110, 18087-18091, doi:10.1073/pnas.1310344110, 2013.
- Dessler, A. E., Schoeberl, M. R., Wang, T., Davis, S. M., Rosenlof, K. H., and Vernier, J. P.: Variations of stratospheric water vapor over the past three decades, *J. Geophys. Res.*, 119, 12588-12598, doi:10.1002/2014jd021712, 2014.
- Ding, Q. H., and Fu, Q.: A warming tropical central Pacific dries the lower stratosphere, *Clim. Dyn.*, 50, 2813-2827, doi:10.1007/s00382-017-3774-y, 2018.
- Flury, T., Wu, D. L., and Read, W. G.: Correlation among cirrus ice content, water vapor and temperature in the TTL as observed by CALIPSO and Aura/MLS, *Atm. Chem. Phys.*, 12, 683-691, doi:10.5194/acp-12-683-2012, 2012.
- Forster, P. M. D., and Shine, K. P.: Stratospheric water vapour changes as a possible contributor to observed stratospheric cooling, *Geophys. Res. Lett.*, 26, 3309-3312, doi:10.1029/1999GL010487, 1999.
- Fueglistaler, S., and Haynes, P. H.: Control of interannual and longer-term variability of stratospheric water vapor, *J. Geophys. Res.*, 110, 14, doi:10.1029/2005jd006019, 2005.
- Fueglistaler, S., Dessler, A. E., Dunkerton, T. J., Folkins, I., Fu, Q., and Mote, P. W.: Tropical tropopause layer, *Rev. Geophys.*, 47, 31, doi:10.1029/2008rg000267, 2009.



- Geller, M. A., Zhou, X. L., and Zhang, M. H.: Simulations of the interannual variability of stratospheric water vapor, *J. Atmos. Sci.*, 59, 1076-1085, doi:10.1175/1520-0469(2002)059<1076:Sotivo>2.0.Co;2, 2002.
- 5 Guttelman, A., Randel, W. J., Massie, S., Wu, F., Read, W. G., and Russell, J. M.: El Nino as a natural experiment for studying the tropical tropopause region, *J. Climate*, 14, 3375-3392, doi:10.1175/1520-0442(2001)014<3375:enoan>2.0.co;2, 2001.
- Held, I. M., and Soden, B. J.: Water vapor feedback and global warming, *Ann. Rev. En. & Env.*, 25, 441-475, doi:10.1146/annurev.energy.25.1.441, 2000.
- 10 Jiang, J. H., Su, H., Zhai, C. X., Perun, V. S., Del Genio, A., Nazarenko, L. S., Donner, L. J., Horowitz, L., Seman, C., Cole, J., Guttelman, A., Ringer, M. A., Rotstayn, L., Jeffrey, S., Wu, T. W., Briant, F., Dufresne, J. L., Kawai, H., Koshiro, T., Watanabe, M., Lecuyer, T. S., Volodin, E. M., Iversen, T., Drange, H., Mesquita, M. D. S., Read, W. G., Waters, J. W., Tian, B. J., Teixeira, J., and Stephens, G. L.: Evaluation of cloud and water vapor simulations in CMIP5 climate models using NASA "A-Train" satellite observations, *J. Geophys. Res.*, 117, 24, doi:10.1029/2011jd017237, 2012.
- 15 Jiang, J. H., Su, H., Zhai, C. X., Wu, L. T., Minschwaner, K., Molod, A. M., and Tompkins, A. M.: An assessment of upper troposphere and lower stratosphere water vapor in MERRA, MERRA2, and ECMWF reanalyses using Aura MLS observations, *J. Geophys. Res.*, 120, 18, doi:10.1002/2015jd023752, 2015.
- 20 John, V. O., and Soden, B. J.: Temperature and humidity biases in global climate models and their impact on climate feedbacks, *Geophys. Res. Lett.*, 34, 5, doi:10.1029/2007gl030429, 2007.
- Liang, C. K., Eldering, A., Guttelman, A., Tian, B., Wong, S., Fetzer, E. J., and Liou, K. N.: Record of tropical interannual variability of temperature and water vapor from a combined AIRS-MLS data set, *J. Geophys. Res.*, 116, 19, doi:10.1029/2010jd014841, 2011.
- 25 Liess, S., and Geller, M. A.: On the relationship between QBO and distribution of tropical deep convection, *J. Geophys. Res.*, 117, 12, doi:10.1029/2011jd016317, 2012.
- Liu, R., Su, H., Liou, K. N., Jiang, J. H., Gu, Y., Liu, S. C., and Shiu, C. J.: An Assessment of Tropospheric Water Vapor Feedback Using Radiative Kernels, *J. Geophys. Res.*, 123, 1499-1509, doi:10.1002/2017jd027512, 2018.
- 30 Livesey, N. J.: EOS Aura MLS Version 4.2x Level 2 data quality and description document, Tech. Rep., D-33509, Rev. A, Jet Propulsion Laboratory, California Institute of Technology, 2015.
- Mote, P. W., Rosenlof, K. H., McIntyre, M. E., Carr, E. S., Gille, J. C., Holton, J. R., Kinnersley, J. S., Pumphrey, H. C., Russell, J. M., and Waters, J. W.: An atmospheric tape recorder: The imprint of



- tropical tropopause temperatures on stratospheric water vapor, *J. Geophys. Res.*, 101, 3989-4006, doi:10.1029/95jd03422, 1996.
- Philander, S. G. H.: El Nino, La Nina, and the Southern Oscillation, International Geophysical Series, Academic Press, San Diego, CA, USA, 293 pp., 1990.
- 5 Randel, W. J., Wu, F., Oltmans, S. J., Rosenlof, K., and Nedoluha, G. E.: Interannual changes of stratospheric water vapor and correlations with tropical tropopause temperatures, *J. Atmos. Sci.*, 61, 2133-2148, doi:10.1175/1520-0469(2004)061<2133:icoswv>2.0.co;2, 2004.
- Randel, W. J., and Jensen, E. J.: Physical processes in the tropical tropopause layer and their roles in a changing climate, *Nature Geosci.*, 6, 169-176, doi:10.1038/ngeo1733, 2013.
- 10 Read, W. G., Lambert, A., Bacmeister, J., Cofield, R. E., Christensen, L. E., Cuddy, D. T., Daffer, W. H., Drouin, B. J., Fetzer, E., Froidevaux, L., Fuller, R., Herman, R., Jarnot, R. F., Jiang, J. H., Jiang, Y. B., Kelly, K., Knosp, B. W., Kovalenko, L. J., Livesey, N. J., Liu, H. C., Manney, G. L., Pickett, H. M., Pumphrey, H. C., Rosenlof, K. H., Sabouchi, X., Santee, M. L., Schwartz, M. J., Snyder, W. V., Stek, P. C., Su, H., Takacs, L. L., Thurstans, R. P., Vomel, H., Wagner, P. A., Waters, J. W., Webster, C. R.,
- 15 Weinstock, E. M., and Wu, D. L.: Aura Microwave Limb Sounder upper tropospheric and lower stratospheric H₂O and relative humidity with respect to ice validation, *J. Geophys. Res.*, 112, 29, doi:10.1029/2007jd008752, 2007.
- Schieferdecker, T., Lossow, S., Stiller, G. P., and von Clarmann, T.: Is there a solar signal in lower stratospheric water vapour?, *Atm. Chem. Phys.*, 15, 9851-9863, doi:10.5194/acp-15-9851-2015, 2015.
- 20 Schwartz, M. J., Waliser, D. E., Tian, B., Wu, D. L., Jiang, J. H., and Read, W. G.: Characterization of MJO-related upper tropospheric hydrological processes using MLS, *Geophys. Res. Lett.*, 35, doi:10.1029/2008gl033675, 2008.
- Soden, B. J., and Held, I. M.: An assessment of climate feedbacks in coupled ocean-atmosphere models, *J. Climate*, 19, 3354-3360, doi:10.1175/jcli3799.1, 2006.
- 25 Soden, B. J., Held, I. M., Colman, R., Shell, K. M., Kiehl, J. T., and Shields, C. A.: Quantifying climate feedbacks using radiative kernels, *J. Climate*, 21, 3504-3520, doi:10.1175/2007jcli2110.1, 2008.
- Solomon, S., Rosenlof, K. H., Portmann, R. W., Daniel, J. S., Davis, S. M., Sanford, T. J., and Plattner, G. K.: Contributions of Stratospheric Water Vapor to Decadal Changes in the Rate of Global Warming, *Science*, 327, 1219-1223, doi:10.1126/science.1182488, 2010.
- 30 Su, H., Neelin, J. D., and Meyerson, J. E.: Mechanisms for lagged atmospheric response to ENSO SST forcing, *J. Climate*, 18, 4195-4215, doi:10.1175/jcli3514.1, 2005.



- Su, H., Read, W. G., Jiang, J. H., Waters, J. W., Wu, D. L., and Fetzer, E. J.: Enhanced positive water vapor feedback associated with tropical deep convection: New evidence from Aura MLS, *Geophys. Res. Lett.*, 33, 5, doi:10.1029/2005gl025505, 2006.
- 5 Takahashi, H., Su, H., and Jiang, J. H.: Error analysis of upper tropospheric water vapor in CMIP5 models using "A-Train" satellite observations and reanalysis data, *Clim. Dyn.*, 46, 2787-2803, doi:10.1007/s00382-015-2732-9, 2016.
- Tao, M. C., Konopka, P., Ploeger, F., Riese, M., Muller, R., and Volk, C. M.: Impact of stratospheric major warmings and the quasi-biennial oscillation on the variability of stratospheric water vapor, *Geophys. Res. Lett.*, 42, 4599-4607, doi:10.1002/2015gl064443, 2015.
- 10 Tian, B., Soden, B. J., and Wu, X. Q.: Diurnal cycle of convection, clouds, and water vapor in the tropical upper troposphere: Satellites versus a general circulation model, *J. Geophys. Res.*, 109, 16, doi:10.1029/2003jd004117, 2004.
- Tian, B., Fetzer, E. J., Kahn, B. H., Teixeira, J., Manning, E., and Hearty, T.: Evaluating CMIP5 models using AIRS tropospheric air temperature and specific humidity climatology, *J. Geophys. Res.*, 118, 114-134, doi:10.1029/2012jd018607, 2013.
- 15 Uma, K. N., Das, S. K., and Das, S. S.: A climatological perspective of water vapor at the UTLS region over different global monsoon regions: observations inferred from the Aura-MLS and reanalysis data, *Clim. Dyn.*, 43, 407-420, doi:10.1007/s00382-014-2085-9, 2014.
- Wallace, J. M., Rasmusson, E. M., Mitchell, T. P., Kousky, V. E., Sarachik, E. S., and von Storch, H.: 20 The structure and evolution of ENSO-related climate variability in the tropical Pacific: Lessons from TOGA, *J. Geophys. Res.*, 103, 14241-14259, doi:10.1029/97jc02905, 1998.
- Wolter, K., and Timlin, M. S.: El Nino/Southern Oscillation behaviour since 1871 as diagnosed in an extended multivariate ENSO index (MEI.ext), *Int. J. Clim.*, 31, 1074-1087, doi:10.1002/joc.2336, 2011.
- Wu, L., Su, H., Jiang, J. H., and Read, W. G.: Hydration or dehydration: competing effects of upper 25 tropospheric cloud radiation on the TTL water vapor, *Atm. Chem. Phys.*, 12, 7727-7735, doi:10.5194/acp-12-7727-2012, 2012.
- Ye, H., Dessler, A. E., and Yu, W. D.: Effects of convective ice evaporation on interannual variability of tropical tropopause layer water vapor, *Atm. Chem. Phys.*, 18, 4425-4437, doi:10.5194/acp-18-4425-2018, 2018.
- 30 Zhou, X. L., Geller, M. A., and Zhang, M. H.: Tropical cold point tropopause characteristics derived from ECMWF reanalyses and soundings, *J. Climate*, 14, 1823-1838, doi:10.1175/1520-0442(2001)014<1823:tcptcd>2.0.co;2, 2001.



Zhou, X. L., Geller, M. A., and Zhang, M. H.: Temperature fields in the tropical tropopause transition layer, *J. Climate*, 17, 2901-2908, doi:10.1175/1520-0442(2004)017<2901:tfittt>2.0.co;2, 2004.

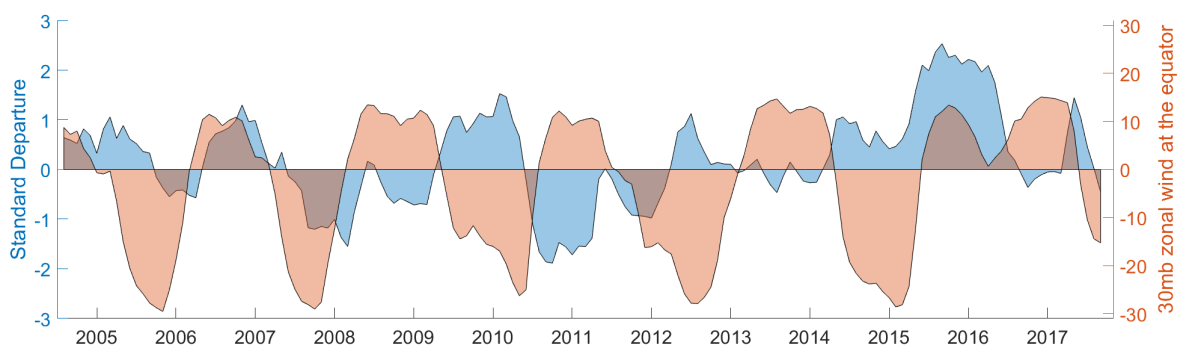
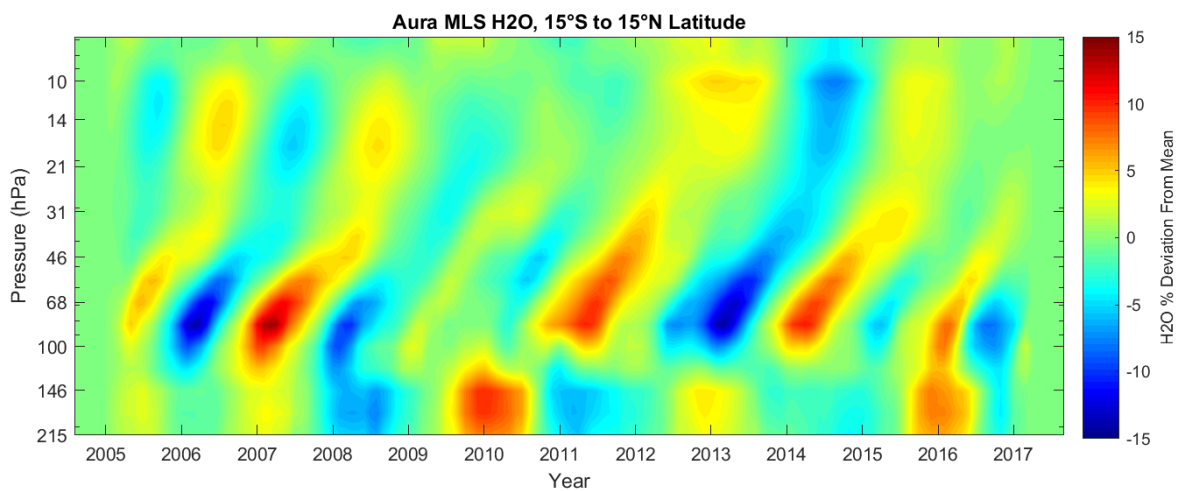


Figure 1. Bimonthly multivariate ENSO index (MEI) (blue) and monthly QBO index based on 30-hPa zonal mean zonal wind at the Equator (u30) (orange) both from NOAA at the period
5 from August 2004 to September 2017. Positive MEI values indicate warm ENSO (El Niño) phases while negative MEI values indicate cold ENSO (La Niña) phases. Positive u30 values denote westerly QBO phases while negative u30 values denote easterly QBO phases.



10 **Figure 2.** Monthly interannual tropical water vapor anomalies from MLS in percentage deviations at different pressure levels from August 2004 to September 2017.

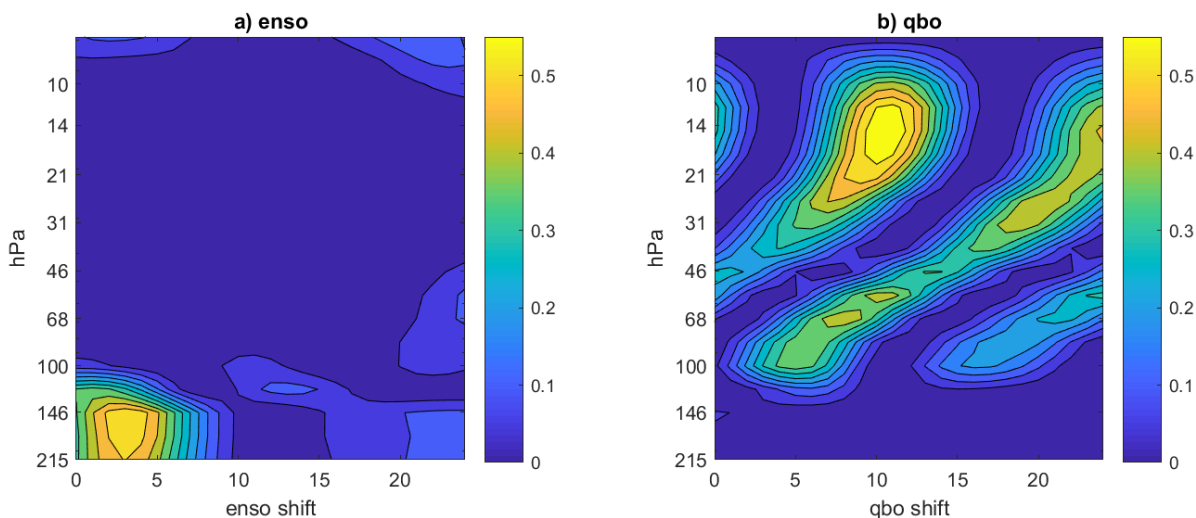


Figure 3. R-squared values for the linear regressions between the interannual tropical water vapor anomalies from MLS and the ENSO or QBO index at each pressure level with time lag shifts from 0-24 months. Figure 3a (left) is for ENSO ($WV = X_0 + X_1 \times \text{ENSO}$) and Fig. 3b (right) is for QBO ($WV = X_0 + X_1 \times \text{QBO}$). The time lag shift indicates the number of months that interannual tropical water vapor anomalies lag the ENSO or QBO index.

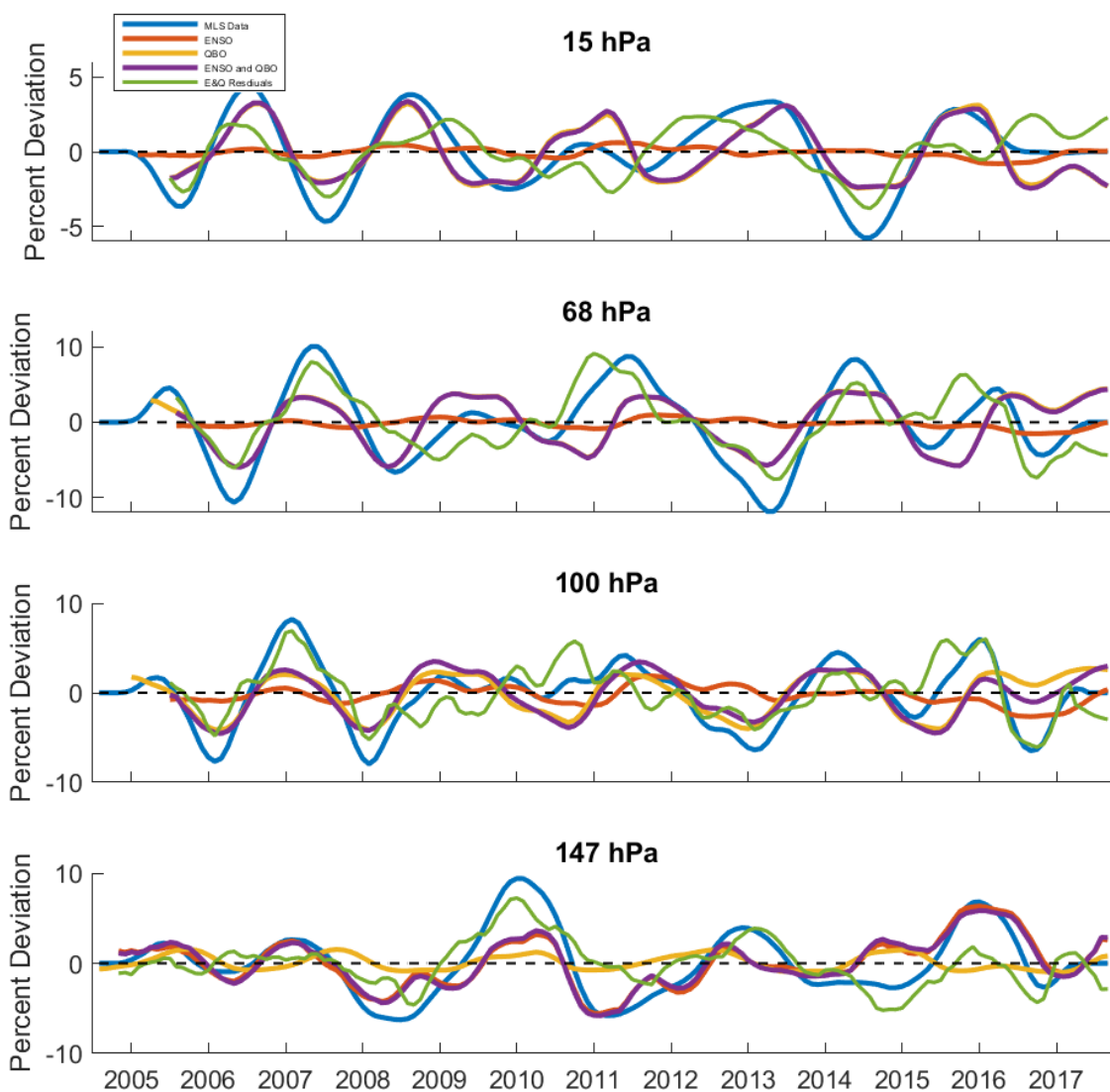


Figure 4. The time series of the monthly interannual tropical water vapor anomalies from MLS (blue lines) and the predicted monthly interannual tropical water vapor anomalies based on the linear regressions on the ENSO index only (red lines), the QBO index only (orange lines), and the ENSO and QBO indices together (purple lines) at the time lag less than 12 months with the highest R-squared value for four specific pressure levels: 15 hPa (top row), 68 hPa (second row), 100 hPa (third row), and 147 hPa (bottom row). The differences between the MLS data (blue lines) and the linear regression lines based on the ENSO and QBO together (purple lines) are also plotted (green lines).

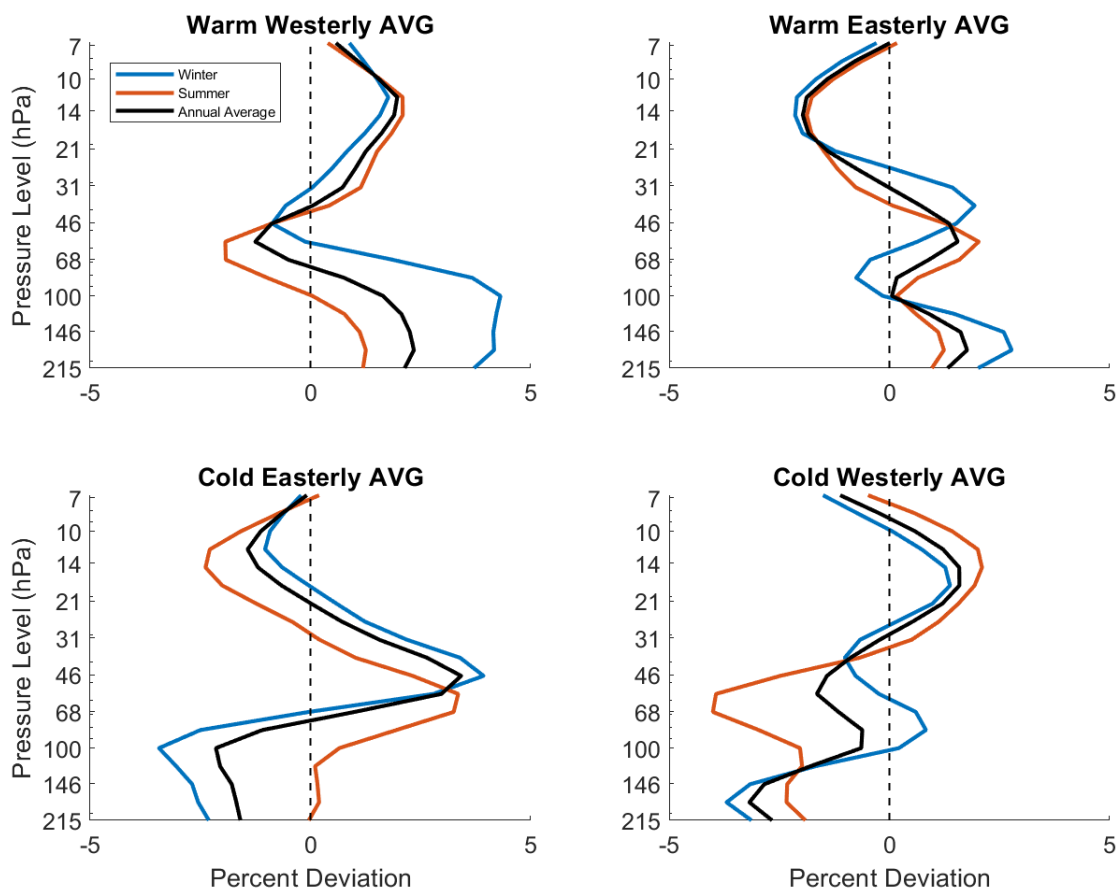


Figure 5. Composite interannual tropical water vapor anomalies from MLS at different pressure levels for winter (NDJFMA) (blue lines), summer (MJJASO) (red lines), and annual (black lines) means at four different cases based on different combinations of ENSO and QBO phases.